Macromolecular Research, Vol. 11, No. 4, pp 260-266 (2003)

EVA/Clay Nanocomposite by Solution Blending: Effect of Aluminosilicate Layers on Mechanical and Thermal Properties

M. Pramanik and S. K. Srivastava*

Department of Chemistry, Indian Institute of Technology, Kharagpur-721302, India

B. K. Samantaray

Department of Physics and Meteorology, Indian Institute of Technology, Kharagpur-721302, India

A. K. Bhowmick

Rubber Technology Centre, Indian Institute of Technology, Kharagpur-721302, India

Received Feb. 8, 2003; Revised Apr. 14, 2003

Abstract: Ethylene vinyl acetate (EVA)/clay nanocomposites were synthesized by blending a solution of ethylene vinyl acetate copolymer containing 12% vinyl acetate abbreviated as EVA-12 in toluene and dispersion of dodecyl ammonium ion intercalated montmorillonite (12Me-MMT) in *N,N*-dimethyl acetamide (DMAc). X-ray patterns of sodium montmorillonite (Na^+-MMT) and 12Me-MMT exhibited $d_{(001)}$ peak at $2\theta = 7.4^\circ$ and $2\theta = 5.6^\circ$ respectively; that is, the interlayer spacing of MMT increased by about 0.39 nm due to intercalation of dodecyl ammonium ions. The XRD trace of EVA showed no peak in the angular range of 3-10° (2θ). In the XRD patterns of EVA/clay hybrids with clay content up to 6 wt% the basal reflection peak of 12Me-MMT was absent, leading to the formation of delaminated configuration of the composites. When the 12Me-MMT content was 8 wt% in the EVA-12 matrix, the hybrid revealed a peak at about $2\theta = 5.6^\circ$, owing to the aggregation of aluminosilicate layers. Transmission electron microscopic photograph exhibited that an average size of 12-15 nm clay layers were randomly and homogeneously dispersed in the polymer matrix, which led to the formation of nanocomposite with delaminated configuration. The formation of delaminated nanocomposites was manifested through the enhancement of mechanical properties and thermal stability, e.g. tensile strength of an hybrid containing only 2 wt% 12Me-MMT was enhanced by about 36% as compared with neat EVA-12.

Keywords: nanocomposite, TEM, SEM, clay minerals, delamination.

Introduction

The development of nanolevel dispersion of clay particles in the polymer matrix has unfolded a new and interesting chapter in the field of materials science in recent years.[1-3] These nanohybrids are two phase materials with unexpected improved properties normally unavailable with the conventional composites or with pure polymers.[4] The extent of improvement is directly related to the aspect ratio and dispersion of the clay layers in the polymer matrix.[5] Depending on the degree or nature of the dispersion of the clay layers in the polymer matrix, either, intercalated nanocomposites where there is regular insertion of the polymer chains in between the clay layers or delaminated nanocomposites where the clay layers are randomly and homogeneously dispersed in the polymer matrix may be obtained.[6] Because of the structural feature, the later type offers the maximum improvement in mechanical and other physical properties of the polymer.[7] The most important aspect of these nanocomposites is that all these improvements are obtained at a very low clay loading in the polymer matrix.[1,8] Clay is not only a chief material but its small amount also provides a high extent of improvement in physicomechanical properties of polymer.[9,10] Because of these reasons, polymer/clay nanocomposites are very important materials today from both the academic and industrial points of view.

Clay minerals are layered materials.[11,12] Among these clay minerals, sodium montmorillonite (Na^+-MMT) has received a great deal of research interest in recent years probably because of its ease to make these organophilic. Na^+-MMT is made organophilic by exchanging the inorganic cations in

*e-mail : sunil111954@yahoo.co.uk

the interlayer space with the organic cations such as alkyl or aryl ammonium ions. The incorporation of such ammonium ions not only changes hydrophilic nature into hydrophobic but also expands the interlayer spacing, which, in turn, depends on the number of carbon atoms in the organic ammonium ions.[13] Montmorillonite without organomodification has been used to develop nanocomposites with polymers such as styrene-acrylonitrile copolymer,[14] acrylonitrile-butadiene rubber[15] etc.; but they are very limited in number, because polymers are to be hydrophilic and sufficiently polar.[9] Organomodified montmorillonite/polymer nanocomposires based on polystyrene,[16] poly(ε-caprolactone),[17] nylon6,[18] polyaniline[19] and Engage rubber[20] etc. have been reported. In most of the cases, polymer/clay nanocomopoites have been synthesized either by melt intercalation method where the molten polymer is blended with clay at a particular temperature related to polymer without using any solvent or by *in-situ* synthesis method where clay is dispersed in the monomer and subsequent polymerization.[21]

Depending on the vinyl acetate content ethylene vinyl acetate (EVA) copolymers are available as rubbers, thermoplastic elastomers and plastics. Wide applications in electrical insulation, cable jacketing and repair, component encapsulation and water proofing, corrosion protection, packaging of components and shoe industry dictate the extent of industrial importance of these polymers.[22] It is now expected that the nanocomposites of these polymers find applications in the same fields with a better performance. In our earlier work, we reported rubber/clay[8,23] nanocomposites which exhibit significant improvement in mechanical and dynamic mechanical properties. EVA-12 containing 12% vinyl acetate is a plastic.[22] In this communication, we report the development of EVA-12/12Me-MMT nanocomposites by solution blending method and the effect of nanolevel dispersion of organoclay on the mechanical and thermal properties of this plastic polymer, EVA-12. The most important excellencies of this method are the probability of both the exfoliation and delamination of aluminosilicate layers in the polymer matrix and the solvent can be reused.

Experimental

Materials. Sodium montmorillonite (Na^+-MMT) clay coded as SWy-2 with a cation exchange capacity 76.4 meq/100 g was supplied by the Clay Mineral Society, University of Missouri, Columbia. Dodecyl amine was purchased from SRL Pvt. Ltd., Mumbai, India. Hydrochloric acid (HCl) with a strength of 37% was taken from E. Merck (India) Ltd. India. The characteristics of ethylene vinyl acetate, (Pilene EVA) used in the development of nanocomposite are summarized in Table I. *N,N*-Dimethyl acetamide (DMAc) was procured from SRL Pvt. Ltd. Mumbai, India and dried by distillation using phosphorous pentoxide. Phosphorous pentoxide (P_2O_5), toluene and dicumyl peroxide (DCP) were obtained from E. Merck (India) Ltd., Mumbai, India; SRL, Mumbai, India and Hercules Inc.(U.S.A.) respectively. The toluene was dried by using Dean-Stark water separator apparatus.

Preparation of Organophilic Montmorillonite. Na^+-MMT was dispersed thoroughly in hot water. A mixture of dodecyl amine, concentrated hydrochloric acid and distilled water was heated for few minutes to obtain a clear solution of dodecyl ammonium chloride. The solution of dodecyl ammonium chloride was added to the dispersion of Na^+-MMT and was subjected to stirring. A white precipitate was obtained after a definite period of stirring, which was filtered and washed twice in hot water under stirring condition to make it free from chloride ions tested by silver nitrate solution. The white product was then dried in a vacuum desiccator. The dried product was ground to the powder form and sieved by a 270 mesh sized sieve.

Preparation of EVA-12/12Me-MMT Nanocomposites. EVA-12 was dissolved in dry toluene under hot and stirring condition in a Witts apparatus. A good dispersion of 12Me-MMT in dry DMAc was prepared in a round bottom flask under the condition as applied for EVA-12. The dispersion of 12Me-MMT was slowly added to EVA-12 solution under stirring at 70-80 °C. Dicumyl peroxide was then mixed with the solution blend and dried at 70 °C under reduced pressure.

TEM Specimen Preparation. A fine capillary tube was dipped in the solution blend of hybrid and few drops were allowed to fall on the surface of clean water. The thin films floated on the water surface were then collected on the Cu grids and dried in vacuum at 70 °C.

Measurements. X-ray diffractograms of the samples were obtained from a Rigaku Miniflex-diffractometer (30 kV, 10 mA) equipped with Cu-K_α-radiation ($\lambda = 0.15418$ nm), with a scanning rate of 2°/min at room temperature. Infrared spectra of all the samples were recorded on Perkin-Elmer 883 over a frequency range of 400 to 4000 cm^{-1}. Scanning electron microscopic (SEM) photograph of the EVA-12/12Me-MMT hybrids were observed on a JEOL (JSM-5800) with an acceleration voltage of 20 kV. Transmission electron micrograph (TEM) of the hybrid was taken with high resolution microscope (CM 12, Philips) with an acceleration voltage of 120 kV. The mechanical properties were mea-

Table I. Source and Characteristics of Ethylene Vinyl Acetate Copolymer

Symbol	Vinyl Acetate Content (wt%)	Source/Company Name	Density (kg/m^3)	Melt Flow Index (dg/min)	Softening Point (°C)
EVA-12	12%	NOCIL, Mumbai, India	933	7	110

sured in a computerized Zwick (model 1445) as per ASTM D 412-97 at an extension rate of 500 mm per minute at room temperature. The impact strength was measured by the instrument, CEAST as per ASTM D 256 with a hammer head of 25 J/m^2 at room temperature. Thermogravimetric analysis was carried out on TG 209, Netzsch with a heating rate of 20°C/minute in nitrogen atmosphere.

Results and Discussion

X-ray Diffraction. The X-ray diffractograms of Na^+-MMT, 12Me-MMT, EVA-12 and its hybrids containing different proportions of 12Me-MMT are displayed in Figure 1. Na^+-MMT shows $d_{(001)}$ peak at an angle 7.4°(2θ) which corresponds to an interlayer spacing of 1.19 nm while 12Me-MMT exhibits the basal reflection peak at $2\theta = 5.6°$ corresponding to an interlayer distance of 1.58 nm. It is therefore clear from the XRD patterns of Na^+-MMT and 12Me-MMT that the intercalation of dodecyl ammonium ions expands gallery gap of MMT as shown in scheme I. In the XRD trace of EVA-12, no peak is observed in the range of the study. The hybrids with 0-6 wt% 12Me-MMT exhibit no peak in the angular range 3-10°(2θ). The disappearance of the 001 reflection peak of the organophilic clay in the hybrids implicates that the aluminosilicate layers of clay are homogeneously exfoliated and randomly dispersed in the EVA-12 copolymer matrix; which, in turn, indicates the formation of delaminated structure of the hybrids. A clear picture of delaminated configuration of the hybrid is depicted through the scheme I. When the organophilic clay content in the hybrids increases to 8 wt%, a peak at an angle close to 5.6°(2θ) is observed because of aggregation of aluminosilicate layers.[5] The delamination of silicate layers of organophilic clay in the EVA-12 matrix is thus possible through the solution blending when the clay content is up to 6 wt%.

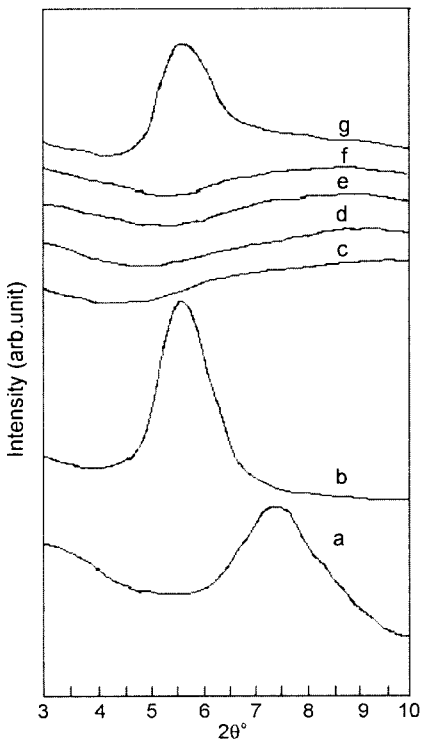

Figure 1. X-ray diffractograms of (a) Na^+-MMT, (b) 12Me-MMT, (c) EVA-12, (d) EVA-12 and 2 wt% 12Me-MMT, (e) EVA-12 and 4 wt% 12Me-MMT, (f) EVA-12 and 6 wt% 12Me-MMT, and (g) EVA-12 and 8 wt% 12Me-MMT.

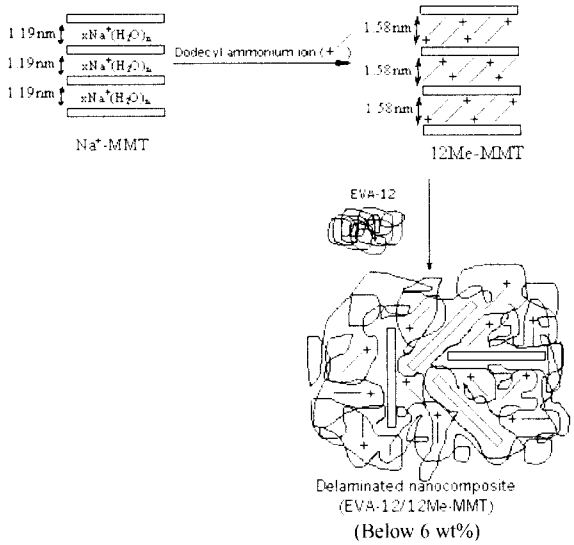

Scheme I. A very short description for the modification Na^+-MMT by dodecyl ammonium ions and the formation delaminated nanocomposite.

Transmissiom Electron Microscopic Photograph of Nanocomposite. Figure 2 shows the transmission electron microscopic (TEM) photograph of the EVA-12/cly hybrid containing 2 wt% organophilic clay. TEM photograph of this composite exhibits that the aluminosilicate layers of MMT are randomly and homogeneously dispersed in the EVA-12 matrix with an average layer thickness 12-15 nm, supporting directly the formation of nanocomposites.

Infrared Spectra. Figure 3 displays the infrared spectra of Na^+-MMT, 12Me-MMT, EVA-12 and its hybrid containing 2 wt% 12Me-MMT. The important bands of all the samples have been assigned in Table II. Na^+-MMT exhibits characteristic bands at around 3638, 3435, 1634, 1044, 526 and 464 cm^{-1} because of the OH stretching of structural hydroxyl groups, -OH stretching of water, -OH deformation of water, Si-O stretching, Al-O-Si deformation and Si-O-Si deformation respectively.[24] The band at around 3435 cm^{-1} is absent in the IR spectrum of 12Me-MMT and at the same time some new bands appear at around 2933 and 2860 cm^{-1} due to the presence of C-H asymmetric stretching of -CH_2 or -CH_3 and C-H symmetric stretching of -CH_2 or -CH_3 respectively.[14]

Figure 2. Transmission electron microscopic photograph of nanocomposite containing 2 wt% 12Me-MMT in EVA-12 matrix.

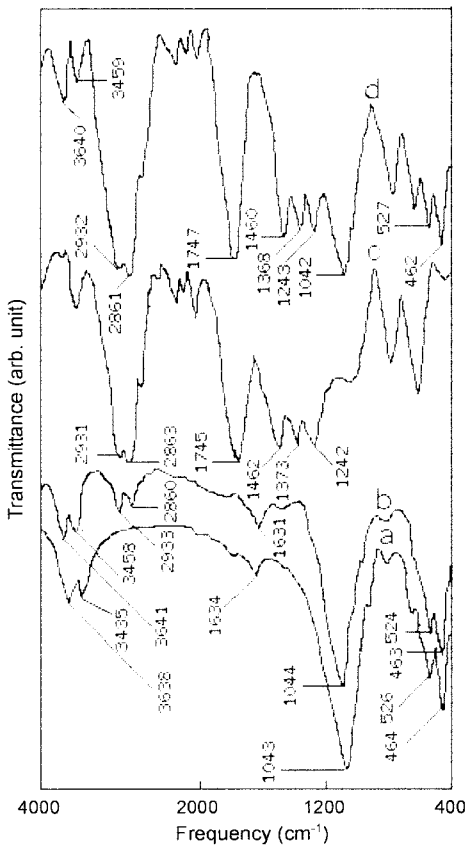

Figure 3. Infrared spectra of (a) Na^+-MMT, (b) 12Me-MMT, (c) EVA-12, and (d) EVA-12 and 2 wt% 12Me-MMT.

Table II. Assignment of Important Bands in the IR Spectrum of Na^+-MMT, 12Me-MMT, Pure EVA-12 and EVA-12/12Me-MMT Hybrids

Observed Band (cm^{-1})	Band Assignment
3641-3638	O-H stretching of structural hydroxyl groups
3435	O-H stretching of water
3459-3458	N-H stretching of NH_3^+
2933-2931	C-H asymmetric stretching of CH_2 or CH_3
2863-2860	C-H symmetric stretching of CH_2 or CH_3
1747-1745	C=O stretching of ester
1634-1631	O-H deformation of water
1462-1460	CH_2 scissoring
1373-1368; 1243-1242	C-O stretching of ester
1044-1042	Si-O stretching
527-524	Al-O-Si deformation
464-462	Si-O-Si deformation

The characteristic band of alkyl ammonium ion is observed in the IR spectrum of 12Me-MMT at around 3458 cm^{-1} for N-H stretching, which is a supporting evidence for the intercalation of dodecyl ammonium ions in between the MMT sheets. EVA-12 and its hybrid with 2 wt% 12Me-MMT reveal a characteristic band of ester corresponding to C=O stretching at around 1747 cm^{-1}. The band at around 1460 cm^{-1} due to the CH_2 scissoring and bands at around 1373, 1243 cm^{-1} for C-O stretching are also observed in the IR spectra of EVA-12 and its hybrid. The characteristic band at 1635 cm^{-1} corresponding to C=O stretching of DMAc is found to be absent both in the EVA-12 and its nanocomposite with 2 wt% 12Me-MMT content, which evidences the absence of entrapped solvent in the nanocomposites. The composites of EVA-12 with 4, 6 and 8 wt% 12Me-MMT content exhibit the features as observed for the hybrid with 2 wt% 12Me-MMT.

Mechanical Properties of EVA-12/Clay Nanocomposites. The mechanical properties of EVA-12/clay nanocomposites prepared have been evaluated through tensile strength, elongation at break and modulus at different elongations. The results are summarized in Figures 4 and 5. It is observed that the tensile strength (TS) as well as the elongation at break (EB) of the composites increase significantly by the introduction of organoclay in the EVA-12 copolymer matrix, as shown in Figure 4. But these enhancements are maximum when the clay content is only 2 wt%. On further increase in the clay content up to 4 wt% in polymer matrix, TS remains almost constant. This improvement in TS and EB of the nanohybrids indicates that the EVA-12 matrix is strengthened by the incorporation of 12Me-MMT dispersed homoge-

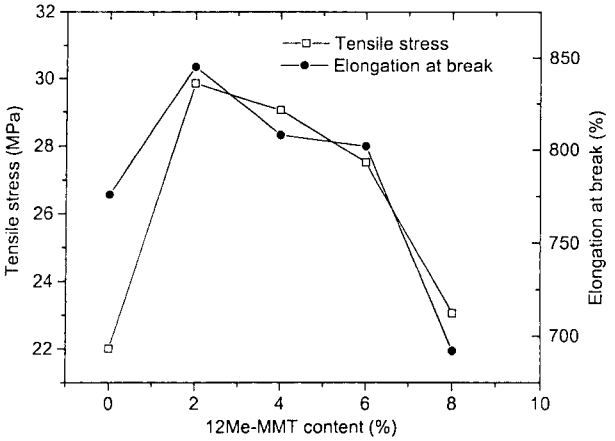

Figure 4. Variation of tensile stress and elongation at break vs. 12Me-MMT content.

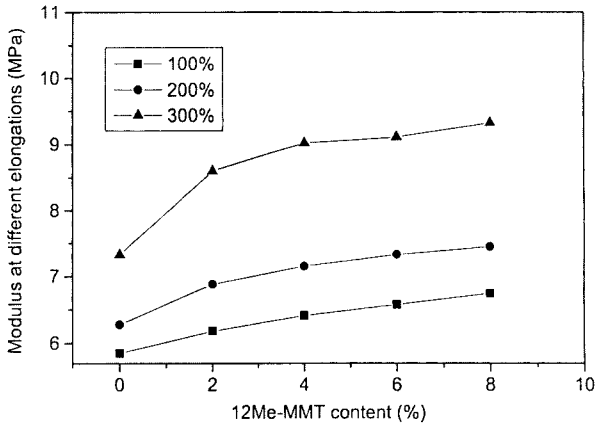

Figure 5. Variation of modulus at different elongations vs. 12Me-MMT content.

neously and randomly in the EVA-12 matrix. The delamination of the aluminosilicate layers (evidenced by XRD shown in Figure 1) of 12Me-MMT to nanolevel in the polymer matrix offers the whole surface of the silicate layers for the strong interaction with the polymer chains. This strong interfacial interaction between polymer chains and nanolevel dispersed layers of 12Me-MMT forms the shear zones when the hybrids are under stress and strain. The formation of such shear zones is distinctly supported by the SEM images of fracture surfaces of the composites containing 0 and 2 wt% organoclay, where, the fracture surface of the composite containing 0 wt% organoclay exhibits some cracks, while, no crack rather some shear zones on the fracture surface of the nanocomposite containing 2 wt% organoclay are observed, as shown in Figure 6. Because of the strong interaction and development of shear zones, TS of the nanocomposites is increased. Increasing the organoclay loading from 4 to 8 wt% in the EVA-12 matrix, it is clearly observed that both the tensile strength and the elongation at break decrease and this decrease in TS and EB is probably due to the aggregation of aluminosilicate layers of clay. This means that the degree of delamination of aluminosilicate layers starts to decrease beyond the 4 wt% filler loading in EVA-12 matrix. The aggregation of organoclay particles in the polymer matrix is evidenced through the XRD of the composite with 8 wt% organoclay. Figure 5 depicts the relationship between modulus at different elongations and organoclay content in the EVA-12 matrix. The modulus at 100, 200 and 300% elongation of the nanocomposites also increase linearly with the organoclay content in the polymer matrix because of the strong interaction of aluminosilicate layers with the polymer chains. EVA/clay nanocomposite[7] prepared by melt intercalation method has shown that the Young's modulus of the nanocomposites increases, but at the same time, both the tensile strength and the elongation at break of the nanocomposites fall. It can also be inferred from the above observations

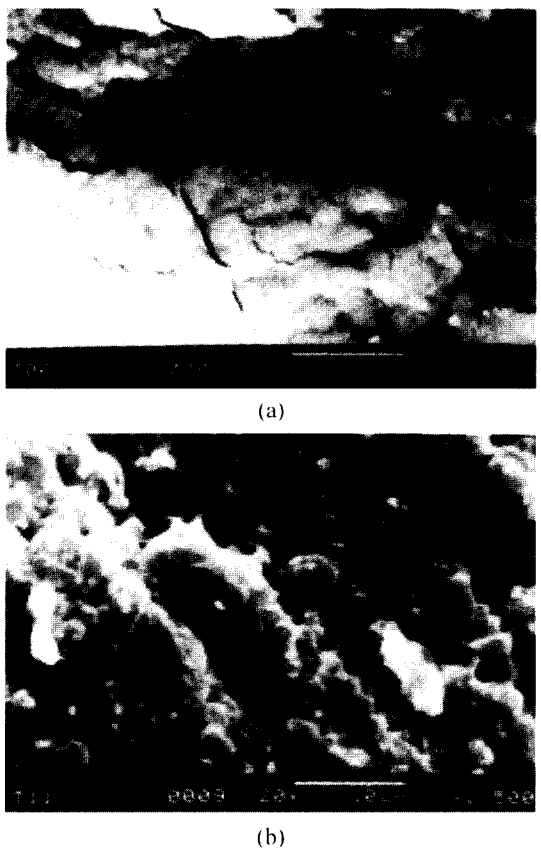

Figure 6. Scanning electron microscopic photographs of fracture surfaces of (a) EVA-12 and (b) nanocomposite containing 2 wt% 12Me-MMT in EVA-12 matrix.

that the EVA-12 copolymer matrix can be strengthened and toughened simultaneously only with 2-4 wt% 12Me-MMT loading through solution blending method. The impact strength of EVA-12 and its hybrids has been summarized in Table III.

Table III. Impact Strength of EVA-12 and Its Nanocomposites

Sample	Tensile Impact (J/m^2)
EVA-12	19.1
EVA-12 + 2 wt% 12Me-MMT	22.2
EVA-12 + 4 wt% 12Me-MMT	22.3
EVA-12 + 6 wt% 12Me-MMT	22.4
EVA-12 + 8 wt% 12Me-MMT	22.6

The impact strength of the control EVA-12 is 19.1 J/m^2. With the incorporation of 2-8 wt% organoclay, the impact strength is greater than 22.1 J/m^2 and the sample did not break. Hence, the impact strength is enhanced by more than 15% even by addition of a small amount of clay due to greater polymer-filler interaction.

Thermal Degradation of Nanocomposites. Figure 7 elucidates the effect of aluminosilicate layers on the thermodegradation of EVA-12. It is clearly noted that the thermal stability of EVA-12 is increased on introduction of 12Me-MMT. The thermal stability of EVA-12/clay hybrid with 2 wt% of 12Me-MMT is relatively more. On further increase in 12Me-MMT loading, the hybrids show a decreasing trend towards their initial thermal decomposition temperature. A two-step weight loss of EVA-12[25] and its hybrids is observed because of two-step decompositions. The first step corresponds to the deacetylation reaction while second one is associated with the formation of transvinylenes accompanied by the main chain scission. The mechanism of this two-step decomposition is represented elsewhere.[25,26] TGA of EVA-12 and its hybrids exhibit that the weight loss in the first step is least when the filler loading is only 2 wt%. The second step weight loss is decreased with increase in filler content. Figure 7 also explicitly shows that the overall weight loss of the hybrids is inversely related to the filler loading; that is, the char formation and the filler loading explicates one to one correspondence because of the high heat resistance exerted by the clay. These findings lead to the fact that the EVA-12 matrix is thermally enhanced for lower filler content (2 wt% 12Me-MMT) because of homogeneous exfoliation and random dispersion of 12Me-MMT on nanometer level. These nanometer level dispersed silicate layers interact strongly with the polymer chains and simultaneously, the barrier effect of silicate layers inhibit the mobility of small molecules produced as a result of thermal degradation. These two effects of silicate layers altogether contribute towards the enhancement of the thermal stability of the nanocomposites. It may be added here that the higher filler loading destabilizes the EVA-12 matrix because of the aggregation of silicate layers (as evidenced through the XRD of hybrid containing 8 wt% 12Me-MMT shown in Figure 1), which ultimately provides a lesser extent of surface area, which, in turn, offers relatively weak interaction with the polymer chains.

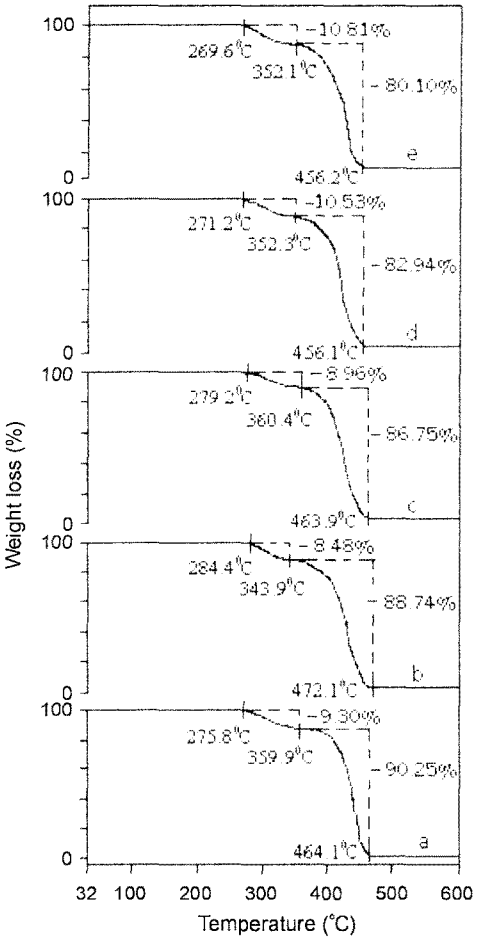

Figure 7. TGA of (a) EVA-12, (b) EVA-12 and 2 wt% 12Me-MMT, (c) EVA-12 and 4 wt% 12Me-MMT, (d) EVA-12 and 6 wt% 12Me-MMT, and (e) EVA-12 and 8 wt% 12Me-MMT.

Conclusions

EVA-12, which is a plastic, can successively be processed to nanocomposite with the introduction of dodecyl ammonium ions intercalated montmorillonite by solution blending method. X-ray diffractograms of the hybrids indicated the formation of delaminated structure. Transmission electron microscopic photograph of the composite exhibited directly the homogeneous and random dispersion of aluminosilicate layers of MMT in the EVA-12 matrix on the range of 12-15 nm. As a result of the formation delaminated nanocomposite EVA-12 matrix was strengthened and toughened simultaneously with 12Me-MMT loading. The homogeneous exfoliation and random dispersion of the aluminosilicate layers yielded a thermally enhanced nanocomposite of EVA-12 with very small 12Me-MMT loading. Therefore, EVA-12/12Me-MMT nanocomposites can be developed very

easily by solution blending method to achieve the better mechanical and thermal properties over neat polymer.

Acknowledgements. The Council of Scientific and Industrial Research (New Delhi, India) is gratefully acknowledged for providing the financial support to carry out this investigation smoothly. The authors are thankful to Dr. T. K. Goswami, Agricultural & Food Engineering, Indian Institute of Technology, Kharagpur, India for carrying out TGA of the samples.

References

(1) A. Okada, M. Kawasumi, A.Usuki, Y. Kojima, T. Kurauchi, and O. Kamigaito, *Mater. Res. Soc. Proc.*, **171**, 45 (1990).
(2) V. Kuppa and E. Manias, *Chem. Mater.*, **14**, 2171 (2002).
(3) M. Kawasumi, N. Hasegawa, M. Kalo, A. Usuki, and A. Okada, *Macromolecules*, **30**, 6333 (1997).
(4) S. Hambir, N. Bulakh, P. Kodgire, R. Kalgaonkar, and J. P. Jog, *J. Polym. Sci., Part B: Polym. Phys.*, **39**, 446 (2001).
(5) J. C. Huang, Z. K. Zhu, X. D. Ma, X. F. Qian, and J. Yin, *J. Mater. Sci.*, **36**, 871 (2001).
(6) M. Alexandre, G. Beyer, C. Henrist, R. Cloots, A. Rulmont, R. Jerome, and P. Dubois, *Macromol. Rapid. Commun.*, **22**, 643 (2001).
(7) X. Kornmann, in Ph. D. Thesis, Lulea University of Technology, 1999.
(8) M. Pramanik, S. K. Srivastava, B. K. Samantary, and A. K. Bhowmick, *J. Appl. Polym. Sci.*, **87**, 2216 (2002).
(9) M. Alexandre, G. Beyer, C. Henrist, R. Cloots, A. Rulmont, R. Jerome, and P. Dubois, *Chem. Mater.*, **13**, 3830 (2001).
(10) X. Kornmann, H. Lindberg, and L. A. Berglund, *Polymer*, **42**, 4493 (2001).
(11) S. K. Srivastava, M. Pramanik, D. Palit, B. K. Mathur, A. K. Kar, B. K. S. Ray, H. Haeuseler, and W. Cordes, *Chem. Mater.*, **13**, 4342 (2001).
(12) G. Lagaly, *Solid State Ionics*, **22**, 43 (1986).
(13) P. Bala, B. K. Samantaray, and S. K. Srivastava, *Mater. Res. Bull.*, **35**, 1717 (2000).
(14) M. H. Noh, L. W. Jang, and D. C. Lee, *J. Appl. Polym. Sci.*, **74**, 179 (1999).
(15) Y. Wu, L. Zhang, Y. Wang, Y. Liang, and D. Yu, *J. Appl. Polym. Sci.*, **82**, 2842 (2001).
(16) T. Wu, S. Hsu, and J. Wu, *J. Polym. Sci., Part B: Polym. Phys.*, **40**, 736 (2002).
(17) M. Tortora, V. Vittora, G. Galli, S. Ritrovati, and E. Chiellim, *Macromol. Mater. Eng.*, **287**, 243 (2002).
(18) X. Liu and Q. Wu, *Polymer*, **43**, 1933 (2002).
(19) W. Jia, E. Segal, D. Kornemandel, Y. Lamhot, M. Narkis, and A. Siegmann, *Synthetic Metals*, **128**, 115 (2002).
(20) S. Ray and A. K. Bhowmick, *Rubber. Chem. Technol.*, **74**, 835 (2001).
(21) Z. Shen, G. P. Siman, and Y. Cheng, *Polymer*, **43**, 4251 (2002).
(22) A. K. Bhowmick and H. L. Stephens, in *Handbook of Elastomers*, 2nd Edition, Marcel Dekker, New York, 2001.
(23) M. Pramanik, S. K. Srivastava, B. K. Samantaray, and A. K. Bhowmick, *J. Mater. Sci. Lett.*, **20**, 1377 (2001).
(24) J. Madejova and P. Komadel, *Clays and Clay Minerals*, **49**, 410 (2001).
(25) S. Dutta, A. K. Bhowmick, P. G. Mukunda, and T. K. Chaki, *Polym. Degrad. Stab.*, **50**, 75 (1995).
(26) M. Zanetti, G. Camino, R. Thomann, and R. Mulhaupt, *Polymer*, **42**, 4501 (2001).